INTERNATIONAL JOURNAL OF
NUMERICAL ANALYSIS AND MODELING
Volume 11, Number 1, Pages 1–23

IMPLICIT ASYMPTOTIC PRESERVING SCHEMES FOR SEMICONDUCTOR BOLTZMANN EQUATION IN THE DIFFUSIVE REGIME

JIA DENG

Abstract. We design several implicit asymptotic-preserving schemes for the linear semiconductor Boltzmann equation with a diffusive scaling, which lead asymptotically to the implicit discretizations of the drift-diffusion equation. The constructions are based on a stiff relaxation step and a stiff convection step obtained by splitting the system equal to the model equation. The one space dimensional schemes are given with the uniform grids and the staggered grids, respectively. The uniform grids are considered only in two space dimension. The relaxation step is evolved with the BGK-penalty method of Filbet and Jin [F. Filbet and S. Jin, J. Comp. Phys. 229(20), 7625-7648, 2010], which avoids inverting the complicated nonlocal anisotropic collision operator. The convection step is performed with a suitable implicit approximation to the convection term, which gives a banded matrix easy to invert. The von-Neumman analysis for the Goldstein-Taylor model show that the one space dimensional schemes are unconditionally stable. The heuristic discussions suggest that all the proposed schemes have the correct discrete drift-diffusion limit. The numerical results verify that all the schemes are asymptotic-preserving. As far as we know, they are the first class of asymptotic-preserving schemes ever introduced for the Boltzmann equation with a diffusive scaling that lead to an implicit discretization of the diffusion limit, thus significantly relax to stability condition.

Key words. linear semiconductor Boltzmann equation, implicit asymptotic-preserving scheme, drift-diffusion limit, BGK-penalty method, time-splitting

1. Introduction

The semiconductor Boltzmann equation, serving as the mathematical model for the highly integrated semiconductor, has a diffusive scaling characterized by the Knudsen number δ (which denotes the ratio of the mean free path of the particle over a typical length) when the electric potential is weak. As $\delta \to 0^+$, the semiconductor Boltzmann equation leads asymptotically to the drift-diffusion equation, which is usually satisfactory for the region having both $\delta \ll 1$ and the initial solution around the local equilibrium state. In practical applications, it is often found that δ varies with very different scale of magnitude within one computational domain and the initial data is in the nonlocal equilibrium state. For the sake of accuracy and efficiency, one usually uses either the domain decomposition type methods [3, 4, 9, 18, 27, 28] or the asymptotic-preserving (AP) schemes [5, 11, 14, 15, 16, 20, 21] to describe the device.

The domain decomposition type methods have the idea of discretizing the kinetic equation in the rarefied regime (where δ is big) and the drift-diffusion equation in the diffusive regime (where $\delta \ll 1$). Such methods generally face the difficulty of determining the locations and the coupling conditions of the interfaces. The AP schemes, on the other hand, solve in the whole computational domain the kinetic equations and hence avoid the problems of interfaces. Specifically, as summarized in [11], an AP scheme possesses the discrete analogy of the continuous asymptotic limit when $\delta \to 0^+$ even with coarse grids Δt, $\Delta x \gg \delta^2$ (where Δt is the time step

Received by the editors May 5, 2012 and, in revised form, March 20, 2013.
2000 *Mathematics Subject Classification.* 82C05, 82D37, 65M12.

and Δx is the space step). A scheme that allows the use of coarse grids should be AP. For kinetic equation with a diffusive scaling, the previous AP schemes need $\Delta t = O(\Delta x^2)$ due to the explicit convection term [5, 11, 14, 15, 16, 20, 21] and typically have the following features [15]:

- The numerical stability is independent of δ. Even in the worst case, it is merely restricted to the parabolic condition $\Delta t \sim O(\Delta x^2)$.
- Given Δt and Δx, the scheme becomes a good explicit solver for the limiting drift-diffusion equation when $\delta \to 0^+$.
- The collision term, though implicit, can be implemented explicitly.

In this paper, we are interested in deriving the implicit AP schemes for the linear semiconductor Boltzmann equation with a diffusive scaling, which improve the first two features above. Specifically, these schemes allow $\Delta t = O(\Delta x)$ instead of $\Delta t = O(\Delta x^2)$ even in the diffusive regime. Moreover, they are good implicit solvers for the limiting drift-diffusion equation as $\delta \to 0^+$ without the electric field, i.e., Δt can be arbitrary for stability. The constructions are based on the BGK-penalty method and a suitable implicit approximation to the convection terms, which have been decoupled through splitting a stiff relaxation step from a stiff convection step. The BGK-penalty method, having the effect of solving the implicit complicated collision term explicitly, was first introduced by Filbet and Jin [7] for a class of hyperbolic system with stiff relaxation source term and the classical Boltzmann equation. The method only requires that the source term has the unique and stable local equilibrium state, and has been applied to the Boltzmann type equations with either the hydrodynamic limit [6, 10, 17] or the diffusive limit [5]. The implicit scheme in the convection step gives the banded matrix easy to invert. Additionally, the velocity discretization is done with the moment method, which has been proved to be stable and convergent in [24].

The paper is arranged as follows. In the next section, we introduce some basic facts about the linear semiconductor Boltzmann equation and its drift-diffusion limit. There we generalize δ to $\delta = \delta(\vec{x}) \in \mathbb{C}^1(\Omega)$, and rewrite the model equation into an equivalent system with respect to the even and odd parities as was done in [14, 16]. The schemes in this paper are actually based on this system. Moreover, the boundary conditions are simply assumed to be periodic. In section 3, we consider one space dimension and derive the implicit AP schemes with the uniform and staggered grids, respectively. For the sake of simplification, we denote the scheme using the uniform grids with IMUG and the other using the staggered grids with IMSG. To construct IMUG and IMSG, we split the system in a suitable way to obtain a stiff relaxation step and a stiff convection step. In the relaxation step, we handle the complicated nonlocal anisotropic collision operator with the BGK-penalty method, which allows the implicit scheme in this step implemented explicitly. The convection step is discretized by a suitable implicit approximation to the convection term, which gives a banded matrix easy to invert and meanwhile allows $\Delta t = O(\Delta x)$ rather than $\Delta t = O(\Delta x^2)$ as in previous approaches. By a comparison, IMSG helps to minimize the bandwith of the matrix in the convection step, while, IMUG has the benefit of easy generalization to the higher space dimension. Through the von-Neumman analysis, IMUG and IMSG are unconditionally stable for the Goldstein-Taylor model. Furthermore, the heuristic discussions suggest that both the one space dimensional schemes are consistent implicit discretiztations of drift-diffusion equation in the asymptotic sense. In section 4 where the electric potential is absent, we extend IMUG to two space dimension and discuss its asymptotic property heuristically. In section 5, the moment method for the velocity

discretization [25] is introduced. Finally, we numerically verify the performance of the schemes in section 6. Our numerical results confirm the AP properties of all the schemes.

2. Linear Semiconductor Boltzmann Equation and its Drift-Diffusion Limit

Consider the electron in the semiconductor. In the situation of parabolic energy band, the dimensionless semiconductor Boltzmann equation has the form of [5]

$$\partial_t f + \vec{v}\cdot\nabla_{\vec{x}} f + \nabla_{\vec{x}}\Phi\cdot\nabla_{\vec{v}} f = \frac{\mathcal{Q}(f)}{\delta}\,. \tag{1}$$

Here the one-particle distribution $f(\vec{x},\vec{v},t)$ describes the probability of electron appearing at position $\vec{x}=(x,y,z)\in\Omega\subset\mathbb{R}^3$ with velocity $\vec{v}=(v_1,v_2,v_3)\in\mathbb{R}^3$ at time $t\in\mathbb{R}^+$. The electric potential $\Phi=\Phi(\vec{x})$ is given explicitly and assumed to be weak, which suggests that the Boltzmann equation has a diffusive scaling. The Knudsen number δ has been generalized to $\delta=\delta(\vec{x})\in\mathbb{C}^1(\Omega)$. In the case of low density approximation, the nonlinear collision operator $\mathcal{Q}$ is reduced to the linear form

$$\begin{aligned}\mathcal{Q}(f)(\vec{v}) &= \textstyle\int_{\mathbb{R}^3}\sigma(\vec{v},\vec{v}')f(\vec{v}')\mathrm{d}\vec{v}'\mathcal{M}(\vec{v}) - \lambda(\vec{v})f(\vec{v})\,,\\ \mathcal{M}(\vec{v}) &= \tfrac{1}{\pi^{3/2}}\exp(-|\vec{v}|^2)\,,\quad \lambda(\vec{v}) = \textstyle\int_{\mathbb{R}^3}\sigma(\vec{v},\vec{v}')\mathcal{M}(\vec{v}')\mathrm{d}\vec{v}'\,,\end{aligned}$$

where $\mathcal{M}(\vec{v})$ is the global Maxwellian, $\lambda(\vec{v})$ is the collision frequency, and $\sigma(\vec{v},\vec{v}')$ is the cross section. In this paper, we assume that σ have been regularized and fulfills

- Rotation invariant: $\forall\mathcal{R}\in\mathbb{SO}(3)$, it holds $\sigma(\mathcal{R}\vec{v},\mathcal{R}\vec{v}')=\sigma(\vec{v},\vec{v}')$. Here $\mathbb{SO}(3)$ denotes the special orthogonal transformation group.
- Symmetric: $\forall\ \vec{v},\vec{v}'\in\mathbb{R}^3$, it holds $\sigma(\vec{v},\vec{v}')=\sigma(\vec{v}',\vec{v})$.
- Bounded: $\exists\ \sigma_0,\sigma_1>0$, such that $\sigma_0\le\sigma(\vec{v},\vec{v}')\le\sigma_1$.

To rescale (1), let $\epsilon=\max_{\vec{x}\in\Omega}\delta(\vec{x})$ and

$$t'=\epsilon t\,,\quad \vec{x}'=\vec{x}\,,\quad \vec{v}'=\vec{v}\,. \tag{2}$$

Inserting (2) into (1), the linear semiconductor Boltzmann equation with a diffusive scaling is obtained as

$$\partial_t f + \frac{1}{\epsilon}(\vec{v}\cdot\nabla_{\vec{x}} f - \vec{E}\cdot\nabla_{\vec{v}} f) = \frac{\mathcal{Q}(f)}{\epsilon\delta}\,, \tag{3}$$

where the subscripts have been omitted and the electric field $\vec{E}=-\nabla_{\vec{x}}\Phi$ is defined. Given the even and odd parities [14, 15, 16]

$$\begin{aligned} r(\vec{x},\vec{v},t) &= \frac{1}{2}[f(\vec{x},\vec{v},t)+f(\vec{x},-\vec{v},t)],\\ j(\vec{x},\vec{v},t) &= \frac{1}{2\epsilon}[f(\vec{x},\vec{v},t)-f(\vec{x},-\vec{v},t)]\,,\end{aligned} \tag{4}$$

it is straightforward that (3) equals to

$$\begin{aligned}\partial_t r + \vec{v}\cdot\nabla_{\vec{x}} j - \vec{E}\cdot\nabla_{\vec{v}} j &= \frac{\mathcal{Q}(r)}{\epsilon\delta}\,,\\ \partial_t j + \frac{\vec{v}\cdot\nabla_{\vec{x}} r - \vec{E}\cdot\nabla_{\vec{v}} r}{\epsilon^2} &= -\frac{\lambda j}{\epsilon\delta}\,.\end{aligned} \tag{5}$$

In the above, the properties $r(\vec{v})=r(-\vec{v}),\ j(\vec{v})=-j(-\vec{v})$, and the rotation invariance including the symmetry of $\sigma(\vec{v},\vec{v}')$ are used. As is known, the mass density ρ and the bulk momentum $\vec{u}=(u_1,u_2,u_3)$ relate to f through

$$\rho(\vec{x},t)=\textstyle\int_{\mathbb{R}^3} f(\vec{x},\vec{v},t)\mathrm{d}\vec{v},\quad \vec{u}(\vec{x},t)=\int_{\mathbb{R}^3}\vec{v}f(\vec{x},\vec{v},t)\mathrm{d}\vec{v}\,.$$

Considering (4), it is clear that

$$\rho(\vec{x},t)=\int_{\mathbb{R}^3} r(\vec{x},\vec{v},t)\mathrm{d}\vec{v},\quad \vec{u}(\vec{x},t)=\epsilon\int_{\mathbb{R}^3}\vec{v}j(\vec{x},\vec{v},t)\mathrm{d}\vec{v}\,.$$

To study the drift-diffusion limit of system (5), we simplify $\delta(x)=\epsilon$ and present some standard properties of $\mathcal{Q}$ [1, 22].

Theorem 2.1. *Denote the Hilbert space* $\mathcal{H}=\mathcal{L}^2\big(\mathbb{R}^3;\mathrm{d}\vec{v}/\mathcal{M}(\vec{v})\big)$ *and the norm* $\|\cdot\|_{\mathcal{H}}=\sqrt{<\cdot,\cdot>_{\mathcal{H}}}$ *with*

$$<f,g>_{\mathcal{H}}=\int_{\mathbb{R}^3} fg\mathcal{M}^{-1}\mathrm{d}\vec{v},\quad \forall f\,,g\in\mathcal{H}\,.$$

Then it holds that

(i) $-\mathcal{Q}$ *is bounded and self-adjoint.*
(ii) $Ker\mathcal{Q}=Span\{\mathcal{M}(\vec{v})\}\subset\mathcal{H}$, $Ran\mathcal{Q}=Ker\mathcal{Q}^{\perp}$.
(iii) *Let* $\vec{h}=\vec{h}(\vec{v})\in\mathbb{R}^3$ *be the unique solution to* $\mathcal{Q}(\vec{h})=\mathcal{M}(\vec{v})\vec{v}$ *in* $\mathrm{Ran}\mathcal{Q}$. *Then* $\vec{h}$ *is an odd function of* $\vec{v}$ *and there exists a positive number* μ *such that* $\int_{\mathbb{R}^3}\vec{v}\otimes\vec{h}\mathrm{d}\vec{v}=-\mu\mathbf{I}_{3\times3}$. μ *is called the mobility.*

When $\epsilon\ll1$, suppose f has the following asymptotic expansion

$$f=f_0+\epsilon f_1+\epsilon^2 f_2+\cdots,$$

and accordingly,

$$\begin{aligned} r&=r_0+\epsilon r_1+\epsilon^2 r_2+\cdots,\\ j&=j_0+\epsilon j_1+\epsilon^2 j_2+\cdots. \end{aligned}\tag{6}$$

Inserting (6) into (5) and equating the different powers of ϵ, thus

$$O(\epsilon^{-2}):\quad \mathcal{Q}(r_0)=0\,,\quad -\lambda j_0=\vec{v}\cdot\nabla_{\vec{x}}r_0-\vec{E}\cdot\nabla_{\vec{v}}r_0\,,\tag{7a}$$

$$O(\epsilon^{-1}):\quad \mathcal{Q}(r_1)=0\,,\quad -\lambda j_1=\vec{v}\cdot\nabla_{\vec{x}}r_1-\vec{E}\cdot\nabla_{\vec{v}}r_1\,,\tag{7b}$$

$$O(\epsilon^{0}):\quad \mathcal{Q}(r_2)=\partial_t r_0+\vec{v}\cdot\nabla_{\vec{x}}j_0-\vec{E}\cdot\nabla_{\vec{v}}j_0\,,\tag{7c}$$

$$O(\epsilon^{1}):\quad \mathcal{Q}(r_3)=\partial_t r_1+\vec{v}\cdot\nabla_{\vec{x}}j_1-\vec{E}\cdot\nabla_{\vec{v}}j_1\,.\tag{7d}$$

Applying the second property in Theorem 2.1 to (7a), there establish $r_0=\rho_0\mathcal{M}\,,r_1=\rho_1\mathcal{M}$ and

$$-\lambda j_0=\vec{v}\mathcal{M}\cdot(\nabla_{\vec{x}}\rho_0+2\rho_0\vec{E})\,,\quad -\lambda j_1=\vec{v}\mathcal{M}\cdot(\nabla_{\vec{x}}\rho_1+2\rho_1\vec{E})\,.$$

The solvability of (7c) suggests

$$\int_{\mathbb{R}^3}(\partial_t r_0+\vec{v}\cdot\nabla_{\vec{x}}j_0-\vec{E}\cdot\nabla_{\vec{v}}j_0)\mathrm{d}\vec{v}=0\,,$$

where

$$\begin{aligned}\int_{\mathbb{R}^3}(\vec{v}\cdot\nabla_{\vec{x}}j_0-\vec{E}\cdot\nabla_{\vec{v}}j_0)\mathrm{d}\vec{v}&=-\nabla_{\vec{x}}\cdot\left[\int_{\mathbb{R}^3}\frac{\vec{v}\otimes\vec{v}\mathcal{M}}{\lambda}\mathrm{d}\vec{v}\cdot(\nabla_{\vec{x}}\rho_0+2\rho_0\vec{E})\right]\\&=-\nabla_{\vec{x}}\cdot\mu(\nabla_{\vec{x}}\rho_0+2\rho_0\vec{E})\,.\end{aligned}\tag{8}$$

The mobility μ in (8) is defined by the third property in Theorem 2.1. Treating (7d) in the same manner as (7c) and setting $\tilde{\rho}=\rho_0+\epsilon\rho_1$, thus $\tilde{\rho}$ satisfies the following drift-diffusion equation

$$\partial_t\tilde{\rho}-\nabla_{\vec{x}}\cdot(\mu\nabla_{\vec{x}}\tilde{\rho}+2\mu\tilde{\rho}\vec{E})=0\,.\tag{9}$$

As a conclusion, there exist $|\vec{u}|\sim O(\epsilon)\,,r-\rho\mathcal{M}\sim O(\epsilon^2)\,,\rho-\tilde{\rho}\sim O(\epsilon^2)$ in the case of $\epsilon\ll1$. For more about the transport equation in the diffusive regime, we refer to [1, 2, 12, 13, 23].

3. Fully Discrete Schemes in One Space Dimension

In one space dimension, (5) is reduced to

$$\partial_t r + v_1 \partial_x j - E\partial_{v_1} j = \frac{\mathcal{Q}(r)}{\epsilon\delta}\,, \tag{10a}$$

$$\partial_t j + \frac{v_1\partial_x r - E\partial_{v_1} r}{\epsilon^2} = -\frac{\lambda j}{\epsilon\delta}\,. \tag{10b}$$

The splitting for (10a)-(10b) consists of

- Relaxation Step:

$$\partial_t r = \frac{\mathcal{Q}(r)}{\epsilon\delta} + E\partial_{v_1} j\,, \tag{11a}$$

$$\partial_t j = \frac{E(\partial_{v_1} r + 2v_1 r)}{\epsilon^2}\,, \tag{11b}$$

- Convection Step:

$$\partial_t r + v_1\partial_x j = 0\,, \tag{12a}$$

$$\partial_t j + \frac{v_1\partial_x r + 2v_1 E r}{\epsilon^2} = -\frac{\lambda j}{\epsilon\delta}\,. \tag{12b}$$

The term $2v_1 Er$ in (11b) ensures the consistence of the relaxation step with the drift-diffusion limit (9), which is the necessary condition for AP . We discretize (11a)-(12b) with the uniform grids and the staggered grids, respectively. In the relaxation step, we employ the BGK-penalty method for the collision term in (11a), where a penalty operator $\mathcal{B}$ is introduced following

$$\mathcal{B}(r) = L(\rho\mathcal{M} - r)\,, \quad L \approx \|D\mathcal{Q}(\rho\mathcal{M})\|_{\mathcal{H}}\,. \tag{13}$$

Here $D\mathcal{Q}(\rho\mathcal{M})$ denotes the Fréchet derivative of $\mathcal{Q}$ and L is a constant. In the convection step, we treat (12a)-(12b) implicitly and apply the central difference method to operator ∂_x.

Without the loss of generality, we restrict the computational domain to $[\,0,\,1\,]$ and chose the grid points $x_i = i\Delta x$, $x_{i\pm\frac{1}{2}} = x_i \pm \frac{\Delta x}{2}$, $\Delta x = 1/N$, $N \in \mathbb{Z}^+$, $i = 0, 1, \cdots, N-1$. Besides, we define

$$\begin{gathered}\theta(x) = \frac{1}{L\Delta t + \epsilon\delta(x)}\,, \quad \tilde{\theta}(x) = \frac{1}{\lambda\Delta t + \epsilon\delta(x)}\,, \quad \gamma(x) = \frac{\delta(x)}{\epsilon}\,, \quad \alpha_1 = \frac{\Delta t}{\Delta x}\,,\\ d(x) = v_1^2\alpha_1^2\gamma(x)\tilde{\theta}(x)\,, \quad c(x) = v_1^2\alpha_1\Delta t\gamma(x)\tilde{\theta}(x)\,.\end{gathered} \tag{14}$$

and

$$\Delta_x j_{\,i} = j_{\,i+\frac{1}{2}} - j_{\,i-\frac{1}{2}}\,, \qquad \Delta_{2x} r_{\,i} = r_{\,i+1} - r_{\,i-1}\,.$$

3.1. Implicit AP Scheme Based on the Uniform Grids (IMUG). We simply denote the scheme using the uniform grids with IMUG. Let the values of the parities at $x_{\,i}$ be

$$r_{\,i}^{\,n} = \frac{1}{\Delta x}\int_{x_{\,i-\frac{1}{2}}}^{x_{i+\frac{1}{2}}} r(x,\vec{v},t^{\,n})\mathrm{d}x\,, \quad j_{\,i}^{\,n} = \frac{1}{\Delta x}\int_{x_{\,i-\frac{1}{2}}}^{x_{i+\frac{1}{2}}} j(x,\vec{v},t^{\,n})\mathrm{d}x\,, \tag{15}$$

The difficulty in the relaxation step is caused by the numerical stiffness contained in the collision term. On one hand, a standard explicit scheme for (11a) requires $\Delta t \sim O(\epsilon\delta)$, which is expensive for $\epsilon\delta \ll 1$. On the other hand, an implicit scheme

for the collision operator is hard to generalize. For example, an explicit-implicit (IMEX) scheme for (11a) is given by

$$\frac{r_i^* - r_i^n}{\Delta t} = \frac{\mathcal{Q}(r_i^*)}{\epsilon\delta_i} + E_i\partial_{v_1} j_i^n \,. \tag{16}$$

When $\mathcal{Q}$ is nonlinear, we have to solve the algebraic system iteratively. While, the BGK-penalty method proposed by Filbet and Jin [7] can ensure this step with an explicit form and a uniform stability condition, simultaneously. The method has the idea of removing the numerical stiffness from $\mathcal{Q}$ to $\mathcal{B}$ firstly, and then solves $\mathcal{Q}$ explicitly. Specifically, we rewrite (11a) into

$$\partial_t r = \frac{\mathcal{Q}(r) - \mathcal{B}(r)}{\epsilon\delta} + \frac{\mathcal{B}(r)}{\epsilon\delta} + E\partial_{v_1} j \,, \tag{17}$$

where the first term on the RHS contains less or even none stiffness compared to the second term owing to $L \approx \|D\mathcal{Q}(\rho\mathcal{M})\|_{\mathcal{H}}$, and thus can be solved explicitly. The first order IMEX for (17) and (11b) is

$$\frac{r_i^* - r_i^n}{\Delta t} = \frac{\mathcal{Q}(r_i^n) - \mathcal{B}(r_i^n)}{\epsilon\delta_i} + \frac{\mathcal{B}(r_i^*)}{\epsilon\delta_i} + E_i\partial_{v_1} j_i^n \,, \tag{18a}$$

$$\frac{j_i^* - j_i^n}{\Delta t} = \frac{E_i(\partial_{v_1} r_i^* + 2v_1 r_i^*)}{\epsilon^2} \,. \tag{18b}$$

From (18a), first note $\rho_i^* = \rho_i^n$, and then use the simple form (13) of $\mathcal{B}$, thus

$$r_i^* = r_i^n + \Delta t\theta_i\mathcal{Q}(r_i^n) + \epsilon\Delta t\delta_i\theta_i E_i\partial_{v_1} j_i^n \,, \tag{19a}$$

$$j_i^* = j_i^n + \frac{\Delta t E_i}{\epsilon^2}(\partial_{v_1} r_i^* + 2v_1 r_i^*) \,. \tag{19b}$$

In the convection step, the fully implicit scheme applied to (12a)-(12b) has the form of

$$\frac{r_i^{n+1} - r_i^*}{\Delta t} + \frac{v_1(j_{i+1}^{n+1} - j_{i-1}^{n+1})}{2\Delta x} = 0 \,, \tag{20a}$$

$$\frac{j_i^{n+1} - j_i^*}{\Delta t} + \frac{v_1(r_{i+1}^{n+1} - r_{i-1}^{n+1})}{2\epsilon^2\Delta x} + \frac{2v_1 E_i r_i^{n+1}}{\epsilon^2} = -\frac{\lambda j_i^{n+1}}{\epsilon\delta_i} \,. \tag{20b}$$

From (20b), one gets

$$j_i^{n+1} = \epsilon\delta_i\tilde{\theta}_i j_i^* - \frac{v_1\alpha_1\gamma_i\tilde{\theta}_i}{2}(r_{i+1}^{n+1} - r_{i-1}^{n+1}) - 2v_1\Delta t\gamma_i\tilde{\theta}_i E_i r_i^{n+1} \,. \tag{21}$$

Inserting (21) into (20a), one obtains

$$\begin{aligned} -\frac{d_{i+1}}{4}r_{i+2}^{n+1} - c_{i+1}E_{i+1}r_{i+1}^{n+1} + \left(1 + \frac{d_{i+1}}{4} + \frac{d_{i-1}}{4}\right) r_i^{n+1} + c_{i-1}E_{i-1}r_{i-1}^{n+1} \\ - \frac{d_{i-1}}{4}r_{i-2}^{n+1} = r_i^* - \epsilon v_1\Delta t\Delta_{2x}\delta_i\tilde{\theta}_i j_i^* \,. \end{aligned} \tag{22}$$

With r_i^{n+1} solved from (22), j_i^{n+1} is finally calculated through (21). Clearly, (22) gives the banded matrix easier to invert compared to (16).

3.2. Stability Analysis. To analyze the stability of IMUG, we assume $\delta(x) = \epsilon$ and consider the Goldstein-Taylor model in one space dimension [8, 26]

$$\frac{\partial f_1}{\partial t} + \frac{1}{\epsilon}\frac{\partial f_1}{\partial x} = \frac{f_{-1} - f_1}{\epsilon^2} \,, \quad \frac{\partial f_{-1}}{\partial t} - \frac{1}{\epsilon}\frac{\partial f_{-1}}{\partial x} = \frac{f_1 - f_{-1}}{\epsilon^2} \,,$$

where the one dimensional velocity variable is given by $v_1 = \pm 1$, and the phase distributions $f_{\pm 1}$ denote $f_1 = f(x,1,t)$, $f_{-1} = f(x,-1,t)$, respectively. The parities are reduced to

$$r = \frac{f_1 + f_{-1}}{2}, \quad j = \frac{f_1 - f_{-1}}{2\epsilon},$$

which leads

$$\partial_t r + \partial_x j = 0, \quad \partial_t j + \frac{\partial_x r}{\epsilon^2} = -\frac{j}{\epsilon^2}. \tag{23}$$

Treating (23) with IMUG, one gets

$$\frac{r_i^{n+1} - r_i^n}{\Delta t} + \frac{j_{i+1}^{n+1} - j_{i-1}^{n+1}}{2\Delta x} = 0, \quad \frac{j_i^{n+1} - j_i^n}{\Delta t} + \frac{r_{i+1}^{n+1} - r_{i-1}^{n+1}}{2\epsilon^2 \Delta x} = -\frac{j_i^{n+1}}{\epsilon^2}. \tag{24}$$

Applying the fourier transform to the spatial variable in (24) and setting $\beta = k\Delta x$, one obtains

$$\hat{r}^{\,n+1} + (\mathrm{i}\alpha_1 \sin\beta)\hat{j}^{\,n+1} = \hat{r}^{\,n}, \quad \mathrm{i}\frac{\alpha_1 \sin\beta}{\epsilon^2}\hat{r}^{\,n+1} + \left(1 + \frac{\Delta t}{\epsilon^2}\right)\hat{j}^{\,n+1} = \hat{j}^{\,n},$$

which equals

$$\begin{bmatrix} \hat{r}^{\,n+1} \\ \hat{j}^{\,n+1} \end{bmatrix} = \frac{1}{1 + \frac{\Delta t}{\epsilon^2} + \frac{\alpha_1^2 \sin^2\beta}{\epsilon^2}} \begin{bmatrix} 1 + \frac{\Delta t}{\epsilon^2} & -\mathrm{i}\alpha_1 \sin\beta \\ -\mathrm{i}\frac{\alpha_1 \sin\beta}{\epsilon^2} & 1 \end{bmatrix} \begin{bmatrix} \hat{r}^{\,n} \\ \hat{j}^{\,n} \end{bmatrix}. \tag{25}$$

By a direct calculation, the two eigenvalues of the matrix on the RHS in (25) are

$$\xi_\pm = \frac{1 + \frac{\Delta t}{2\epsilon^2} \pm \frac{\Delta t}{2\epsilon^2}\sqrt{1 - \frac{4\epsilon^2 \sin^2\beta}{\Delta x^2}}}{1 + \frac{\Delta t}{\epsilon^2} + \frac{\alpha_1^2 \sin^2\beta}{\epsilon^2}}.$$

If $\xi_\pm \in \mathbb{R}$, then

$$|\xi_\pm| \le \frac{1 + \frac{\Delta t}{2\epsilon^2} + \frac{\Delta t}{2\epsilon^2}}{1 + \frac{\Delta t}{\epsilon^2} + \frac{\alpha_1^2}{\epsilon^2}\sin^2\beta} = \frac{1 + \frac{\Delta t}{\epsilon^2}}{1 + \frac{\Delta t}{\epsilon^2} + \frac{\alpha_1^2 \sin^2\beta}{\epsilon^2}} \le 1.$$

If $\xi_\pm \in \mathbb{C}$, then

$$|\xi_\pm|^2 = \frac{1 + \frac{\Delta t^2}{4\epsilon^4} + \frac{\Delta t}{\epsilon^2} + \frac{\Delta t^2}{4\epsilon^4}\left(\frac{4\epsilon^2 \sin^2\beta}{\Delta x^2} - 1\right)}{\left(1 + \frac{\Delta t}{\epsilon^2} + \frac{4\alpha_1^2}{\epsilon^2}\sin^2\beta\right)^2} = \frac{1}{1 + \frac{\Delta t}{\epsilon^2} + \frac{\alpha_1^2 \sin^2\beta}{\epsilon^2}} \le 1.$$

As a conclusion, the two eigenvalues always satisfy $|\xi_\pm| \le 1$, and thus IMUG is unconditionally stable for any Δt, Δx, $\epsilon > 0$.

3.3. Implicit AP Scheme Based on the Staggered Grids (IMSG). To minimize the bandwith of the matrix in the convection step, we reformulate the scheme using the staggered grids. Define

$$r_i^n = \frac{1}{\Delta x}\int_{x_{i-\frac{1}{2}}}^{x_{i+\frac{1}{2}}} r(x,\vec{v},t^{\,n})\mathrm{d}x, \quad j_{i+\frac{1}{2}}^n = \frac{1}{\Delta x}\int_{x_i}^{x_{i+1}} j(x,\vec{v},t^{\,n})\mathrm{d}x.$$

Applying IMSG to (11a)-(12b), one gets

- Relaxation Step:

$$\begin{aligned} &\frac{r_i^* - r_i^n}{\Delta t} = \frac{\mathcal{Q}(r_i^{\,n}) - \mathcal{B}(r_i^{\,n})}{\epsilon\delta_i} + \frac{\mathcal{B}(r_i^*)}{\epsilon\delta_i} + \frac{E_{i-\frac{1}{2}}\partial_{v_1} j_{i-\frac{1}{2}}^n + E_{i+\frac{1}{2}}\partial_{v_1} j_{i+\frac{1}{2}}^n}{2}, \\ &\frac{j_{i+\frac{1}{2}}^* - j_{i+\frac{1}{2}}^n}{\Delta t} = \frac{E_i(\partial_{v_1} r_i^* + 2v_1 r_i^*) + E_{i+1}(\partial_{v_1} r_{i+1}^* + 2v_1 r_{i+1}^*)}{2\epsilon^2}, \end{aligned} \tag{26}$$

- Convection Step:

$$\frac{r_i^{n+1}-r_i^*}{\Delta t}+\frac{v_1(j_{i+\frac12}^{n+1}-j_{i-\frac12}^{n+1})}{\Delta x}=0\,, \tag{27a}$$

$$\frac{j_{i+\frac12}^{n+1}-j_{i+\frac12}^*}{\Delta t}+\frac{v_1(r_{i+1}^{n+1}-r_i^{n+1})}{\epsilon^2\Delta x}+\frac{v_1E_ir_i^{n+1}+E_{i+1}r_{i+1}^{n+1}}{\epsilon^2}=-\frac{\lambda j_{i+\frac12}^{n+1}}{\epsilon\delta_{i+\frac12}}\,, \tag{27b}$$

where the mid-point formula are applied. For example, the term $E\partial_{v_1}r$ at $x_{i+\frac12}$ is approximated by

$$E_{i+\frac12}\partial_{v_1}r_{i+\frac12}=\frac{E_i\partial_{v_1}r_i+E_{i+1}\partial_{v_1}r_{i+1}}{2}\,.$$

From (26), one obtains

$$r_i^*=r_i^n+\Delta t\theta_i\,\mathcal{Q}(r_i^n)+\frac{\epsilon\Delta t\delta_i\theta_i}{2}(E_{i-\frac12}\partial_{v_1}j_{i-\frac12}^n+E_{i+\frac12}\partial_{v_1}j_{i+\frac12}^n)\,, \tag{28a}$$

$$j_{i+\frac12}^*=j_{i+\frac12}^n+\frac{\Delta t}{2\epsilon^2}[E_i(\partial_{v_1}r_i^*+2v_1r_i^*)+E_{i+1}(\partial_{v_1}r_{i+1}^*+2v_1r_{i+1}^*)]\,. \tag{28b}$$

Through (27b), one gets

$$\begin{aligned}j_{i+\frac12}^{n+1}=\epsilon(\delta\tilde\theta j^*)_{i+\frac12}-v_1\alpha_1(\gamma\tilde\theta)_{i+\frac12}(r_{i+1}^{n+1}-r_i^{n+1})\\ -v_1\Delta t(\gamma\tilde\theta)_{i+\frac12}(E_ir_i^{n+1}+E_{i+1}r_{i+1}^{n+1})\,,\end{aligned} \tag{29}$$

which leads (27a) to

$$\begin{aligned}-(d_{i+\frac12}+c_{i+\frac12}E_{i+1})r_{i+1}^{n+1}+(1+d_{i+\frac12}+d_{i-\frac12}-c_{i+\frac12}E_i+c_{i-\frac12}E_i)r_i^{n+1}\\ -(d_{i-\frac12}-c_{i-\frac12}E_{i-1})r_{i-1}^{n+1}=r_i^*-\epsilon v_1\Delta t\Delta_x(\delta\tilde\theta j^*)_i\,.\end{aligned} \tag{30}$$

With r_i^{n+1} solved from (30), $j_{i+\frac12}^{n+1}$ is then calculated according to (29). Compared with the five-point scheme (22), the three-point scheme (30) has a smaller bandwith. Applying IMSG to system (23), one can justify the uniform stability as well as IMUG. We omit the simple details.

3.4. The Asymptotic Property. While we can not prove a general AP property for either scheme, here we can compare the limiting behavior of the two schemes in the asymptotic sense. We still assume $\delta(x)=\epsilon$. As $\epsilon\to0^+$, if IMUG approaches the local Maxwellian, i.e., $r_i^{n+1}=\rho_i^{n+1}\mathcal{M}+O(\epsilon^2)$, then (21) gives

$$j_i^{n+1}=-\frac{v_1\mathcal{M}}{2\lambda\Delta x}\Delta_{2x}\rho_i^{n+1}-\frac{2v_1\mathcal{M}}{\lambda}E_i\rho_i^{n+1}+O(\epsilon^2)\,.$$

Applying these to (20a) and ignoring $O(\epsilon^2)$ term, one gets

$$\frac{\rho_i^{n+1}\mathcal{M}-r_i^*}{\Delta t}-\frac{v_1^2\mathcal{M}}{\lambda}\frac{\rho_{i+2}^{n+1}-2\rho_i^{n+1}+\rho_{i-2}^{n+1}}{4\Delta x^2}-\frac{v_1^2\mathcal{M}}{\lambda}\frac{E_{i+1}\rho_{i+1}^{n+1}-E_{i-1}\rho_{i-1}^{n+1}}{\Delta x}=0\,. \tag{31}$$

Integrating (31) with $\vec v$ over $\mathbb{R}^3$ and using the property $\rho_i^*=\rho_i^n$ in the relaxation step, (31) is actually the five-point scheme for the drift-diffusion equation (9). Similarly, IMSG has the discrete diffusion limit as

$$\frac{\rho_i^{n+1}\mathcal{M}-r_i^*}{\Delta t}-\frac{v_1^2\mathcal{M}}{\lambda}\frac{\rho_{i+1}^{n+1}-2\rho_i^{n+1}+\rho_{i-1}^{n+1}}{\Delta x^2}-\frac{v_1^2\mathcal{M}}{\lambda}\frac{E_{i+1}\rho_{i+1}^{n+1}-E_{i-1}\rho_{i-1}^{n+1}}{\Delta x}=0\,,$$

which is three-point scheme for (9). Three point scheme is clearly better than five-point one for the drift-diffusion equation, since the latter needs twice as many grid

points as the former to achieve the same error. On the other hand, in contrast with IMUG, it is not straightforward to extend IMSG to two space dimension, when the scheme should possess not only the compact stencil (three point scheme in each space dimension) but also the AP property. For example, to evolve r, one would need $r_{i,k}$, $j_{i\pm1/2,k}$ and $j_{i,k\pm1/2}$, whereas, it becomes confusing where to discretize j, at $(i\pm1/2,k)$ or $(i,k\pm1/2)$? One might approximate these by the points corresponding to the integer indices, but one will lose the compactness of the stencil. If one does not do that, it seems one needs to involve both $j_{i\pm1/2,k}$ and $j_{i,k\pm1/2}$ by two equations for j. Then what about AP? The situation is even more intricate when the electric field and the Knudsen number are not constant. How to do it needs a very careful study. Anyway it is not straightforward and left to a future work.

4. Fully Discrete Scheme in Two Space Dimension with $\Phi(\vec{x})=0$

Without loss of generality, we simply assume $\delta(x)=\epsilon$. Consequently, system (5) in two space dimension and $\Phi(\vec{x})=0$ is reduced to

$$\partial_t r + v_1\partial_x j + v_2\partial_y j = \frac{\mathcal{Q}(r)}{\epsilon^2}\,,\quad \partial_t j + \frac{v_1\partial_x r + v_2\partial_y r}{\epsilon^2} = -\frac{\lambda j}{\epsilon^2}\,. \tag{32}$$

We extend IMUG to (32). The splitting for (32) consists of

- Relaxation Step:

$$\partial_t r = \frac{\mathcal{Q}(r)}{\epsilon^2}\,,\quad \partial_t j = 0\,, \tag{33}$$

- Convection Step:

$$\partial_t r + v_1\partial_x j + v_2\partial_y j = 0\,,\quad \partial_t j + \frac{v_1\partial_x r + v_2\partial_y r}{\epsilon^2} = -\frac{\lambda j}{\epsilon^2}\,. \tag{34}$$

Let the computational domain be $\Omega=[\,0,\,1\,]\times[\,0,\,1\,]$ and the grid points be $x_{\,i}=i\Delta x\,, y_{\,l}=l\Delta y$, $\Delta x=\Delta y=1/N$, $N\in\mathbb{Z}^+$, $i\,,l=0,1,\cdots,N-1$. The values of the parities are defined at $(x_{\,i},\,y_{\,l})$ through

$$r^{\,n}_{\,i,l} = \frac{1}{\Delta x\Delta y}\int_{x_{\,i-\frac{1}{2}}}^{x_{i+\frac{1}{2}}}\int_{y_{\,l-\frac{1}{2}}}^{y_{l+\frac{1}{2}}} r(x,y,\vec{v},t^{\,n})\mathrm{d}x\mathrm{d}y\,,$$
$$j^{\,n}_{\,i,l} = \frac{1}{\Delta x\Delta y}\int_{x_{\,i-\frac{1}{2}}}^{x_{i+\frac{1}{2}}}\int_{y_{\,l-\frac{1}{2}}}^{y_{l+\frac{1}{2}}} j(x,y,\vec{v},t^{\,n})\mathrm{d}x\mathrm{d}y\,.$$

Considering (33)-(34), IMUG takes the form of

- Relaxation Step:

$$\frac{r^{\,*}_{\,i,l}-r^{\,n}_{\,i,l}}{\Delta t} = \frac{\mathcal{Q}(r^{\,n}_{\,i,l})-\mathcal{B}(r^{\,n}_{\,i,l})}{\epsilon^2} + \frac{\mathcal{B}(r^{\,*}_{\,i,l})}{\epsilon^2}\,,\quad j^{\,*}_{\,i,l}=j^{\,n}_{\,i,l}\,,$$

- Convection Step:

$$\frac{r^{\,n+1}_{\,i,l}-r^{\,*}_{\,i,l}}{\Delta t} + \frac{v_1(j^{\,n+1}_{\,i+1,l}-j^{\,n+1}_{\,i-1,l})}{2\Delta x} + \frac{v_2(j^{\,n+1}_{\,i,l+1}-j^{\,n+1}_{\,i,l-1})}{2\Delta y} = 0\,, \tag{35a}$$

$$\frac{j^{\,n+1}_{\,i,l}-j^{\,*}_{\,il}}{\Delta t} + \frac{v_1(r^{\,n+1}_{\,i+1,l}-r^{\,n+1}_{\,i-1,l})}{2\epsilon^2\Delta x} + \frac{v_2(r^{\,n+1}_{\,i,l+1}-r^{\,n+1}_{\,i,l-1})}{2\epsilon^2\Delta y} = -\frac{\lambda j^{\,n+1}_{\,i,l}}{\epsilon^2}\,. \tag{35b}$$

Let

$$\alpha_2=\Delta t/\Delta y\,,\quad \tilde{d}_1=v_1^2\alpha_1^2\tilde{\theta}\,,\quad \tilde{d}_2=v_2^2\alpha_2^2\tilde{\theta}\,,\quad \tilde{d}_3=v_1v_2\alpha_1\alpha_2\tilde{\theta}\,,$$

where $\tilde{\theta}(\vec{x})$ and $\theta(\vec{x})$ given by (14) have been reduced to the constants $\tilde{\theta} = (\lambda\Delta t + \epsilon^2)^{-1}$ and $\theta = (L\Delta t + \epsilon^2)^{-1}$, respectively. The relaxation step gives r_i^* and j_i^* as

$$r_{i,l}^* = r_{i,l}^n + \Delta t\theta\mathcal{Q}(r_{i,l}^n)\,, \quad j_{i,l}^* = j_{il}^n\,. \tag{36}$$

While, (35b) in the convection step suggests

$$j_{i,l}^{n+1} = \epsilon^2\tilde{\theta}j_{i,l}^* - \frac{v_1\alpha_1\tilde{\theta}}{2}\Delta_{2x}r_{i,l}^{n+1} - \frac{v_2\alpha_2\tilde{\theta}}{2}\Delta_{2y}r_{i,l}^{n+1}\,, \tag{37}$$

which leads (35a) to

$$\left(1 + \frac{\tilde{d}_1}{2} + \frac{\tilde{d}_2}{2}\right) r_{i,l}^{n+1} - \frac{\tilde{d}_1}{4}(r_{i+2,l}^{n+1} + r_{i-2,l}^{n+1}) - \frac{\tilde{d}_2}{4}(r_{i,l+2}^{n+1} + r_{i,l-2}^{n+1}) - \frac{\tilde{d}_3}{2}(r_{i+1,1+1}^{n+1} - r_{i-1,l+1}^{n+1} - r_{i+1,l-1}^{n+1} + r_{i-1,l-1}^{n+1}) = g_{i,l}^*\,, \tag{38}$$

with

$$g_{i,l}^* = r_{i,l}^* - \frac{\epsilon^2 v_1\alpha_1\tilde{\theta}}{2}\Delta_{2x}j_{i,l}^* - \frac{\epsilon^2 v_2\alpha_2\tilde{\theta}}{2}\Delta_{2y}j_{i,l}^*\,.$$

Here, the discrete operators Δ_{2x} and Δ_{2y} are defined by

$$\Delta_{2x}r_{i,l} = r_{i+1,l} - r_{i-1,l}\,, \quad \Delta_{2y}r_{i,l} = r_{i,l+1} - r_{i,l-1}\,.$$

Note, the system (38) is actually not difficult to solve due to its sparse and banded coefficient matrix.

4.1. The Asymptotic Property. When $\epsilon \to 0^+$, if $r_{i,l}^{n+1} = \rho_{i,l}^{n+1}\mathcal{M} + O(\epsilon^2)$. Applying (37) to (35a) and ignoring $O(\epsilon^2)$ term, one obtains the discrete diffusion limit

$$\frac{\rho_{i,l}^{n+1}\mathcal{M} - r_{i,l}^*}{\Delta t} - \frac{v_1^2\mathcal{M}}{\lambda}\frac{\rho_{i+2,l}^{n+1} - 2\rho_{i,l}^{n+1} + \rho_{i-2,l}^{n+1}}{4\Delta x^2} - \frac{v_2^2\mathcal{M}}{\lambda}\frac{\rho_{i,l+2}^{n+1} - 2\rho_{i,l}^{n+1} + \rho_{i,l-2}^{n+1}}{4\Delta y^2} - \frac{v_1v_2\mathcal{M}}{\lambda}\frac{\rho_{i+1,1+1}^{n+1} - \rho_{i-1,l+1}^{n+1} - \rho_{i+1,l-1}^{n+1} + \rho_{i-1,l-1}^{n+1}}{2\Delta x\Delta y} = 0\,. \tag{39}$$

Integrating (39) with $\vec{v}$ over R^3 and using the property $\rho_{i,l}^* = \rho_{i,l}^n$ in the relaxation step, one gets an implicit discretization for the diffusion equation.

5. Velocity Discretization

The moment method for velocity discretization mainly uses one dimensional Hermite polynomial $h_{m_1}(v_1)$, $v_1 \in \mathbb{R}$, $m_1 \in \mathbb{Z}_0^+$, which satisfies

$$h_{-1}(v) = 0, \quad h_0(v) = \pi^{-1/4}, \tag{40a}$$

$$h_{m_1+1}(v) = v\sqrt{\frac{2}{m_1+1}}h_{m_1}(v) - \sqrt{\frac{m_1}{m_1+1}}h_{m_1-1}(v)\,,\ m_1 \geq 0, \tag{40b}$$

$$h'_{m_1}(v) = \sqrt{2m_1}\,h_{m_1-1}(v). \tag{40c}$$

Introducing the triple index $\mathbf{m} = (m_1, m_2, m_3)$, $m_1, m_2, m_3 \in \mathbb{Z}_0^+$ and setting [24, 25]

$$h_{\mathbf{m}}(\vec{v}) = h_{m_1}(v_1)h_{m_2}(v_2)h_{m_3}(v_3)\,, \quad v_1\,, v_2\,, v_3 \in \mathbb{R}\,,$$

the series $\{h_{\mathbf{m}}(\vec{v})\mathcal{M}(\vec{v})\}_{\mathbf{m}}$ forms an orthonormal basis of the Hilbert space $\mathcal{H}$. As was done in [14, 19], we factor the Maxwellian from the parities

$$r = \varphi(\vec{x}, \vec{v}, t)\mathcal{M}(\vec{v}), \quad j = \psi(\vec{x}, \vec{v}, t)\mathcal{M}(\vec{v}), \tag{41}$$

where

$$\varphi = \sum_{0\le \mathbf{m}\le \mathbf{M}} \varphi_{\mathbf{m}}(\vec{x},t)h_{\mathbf{m}}(\vec{v}), \quad \psi = \sum_{0\le \mathbf{m}\le \mathbf{M}} \psi_{\mathbf{m}}(\vec{x},t)h_{\mathbf{m}}(\vec{v})\,. \tag{42}$$

For the sake of numerical implementations, the orthonormal basis in (42) has been truncated for a specified triple index $\mathbf{M} = (M_1, M_2, M_3)$, $M_1, M_2, M_3 \in \mathbb{Z}^+$. Additionally, the relation $0 \le \mathbf{m} \le \mathbf{M}$ denotes $0 \le m_i \le M_i\,, i = 1, 2, 3$. From (41), one has

$$\nabla_{\vec{v}} r = \mathcal{M}\nabla_{\vec{v}}\varphi - 2\vec{v}\varphi\mathcal{M},\ \nabla_{\vec{v}} j = \mathcal{M}\nabla_{\vec{v}}\psi - 2\vec{v}\psi\mathcal{M}.$$

As an example, we discretize $\partial_{v_1} r$ only. Using the property (40c), one gets

$$\partial_{v_1}\varphi = \sum_{0\le \mathbf{m}\le \mathbf{M}-\mathbf{e}_1} \sqrt{2(m_1+1)}\varphi_{\mathbf{m}+\mathbf{e}_1} h_{\mathbf{m}}(\vec{v})\,, \tag{43}$$

where $\mathbf{e}_1 = (1, 0, 0)$. Expanding $\varphi_{\mathbf{m}}$ following

$$\varphi_{\mathbf{m}} = \int_{\mathbb{R}^3} \varphi(\vec{v}')h_{\mathbf{m}}(\vec{v}')e^{-|\vec{v}'|^2}\mathrm{d}\vec{v}' = \sum_{0\le \mathbf{l}\le \mathbf{M}} \varphi(\vec{v}^{\mathbf{l}})h_{\mathbf{m}}(\vec{v}^{\mathbf{l}})\omega^{\mathbf{l}}\,,$$

and applying it to (43), thus

$$\partial_{v_1}\varphi(\vec{v}) = \sum_{0\le \mathbf{l},\mathbf{m}\le \mathbf{M}-\mathbf{e}_1} \sqrt{2(m_1+1)}h_{\mathbf{m}}(\vec{v})h_{\mathbf{m}+\mathbf{e}_1}(\vec{v}^{\mathbf{l}})\omega^{\mathbf{l}}\varphi(\vec{v}^{\mathbf{l}})\,.$$

Here, $v_i^{l_i}$ denotes the l_i-th root of the one-dimensional M_i+1-th order Hermite polynomial $h_{M_i+1}(v_i)$ with $0 \le l_i \le M_i\,, i = 1, 2, 3$, the associated weight $\omega^{\mathbf{l}}$ has the form of

$$\omega^{\mathbf{l}} = \prod_{i=1}^{3} \frac{1}{(M_i+1)h_{M_i}^2(v_i^{l_i})}\,. \tag{44}$$

Finally, the collision term is evaluated by

$$\begin{aligned}\mathcal{Q}(r)(\vec{v}) &= \mathcal{M}(\vec{v})\int_{\mathbb{R}^3} \sigma(\vec{v},\vec{v}')\varphi(\vec{v}')\mathcal{M}(\vec{v}')\mathrm{d}\vec{v}' - \lambda(\vec{v})r(\vec{v})\\ &= \pi^{-3/2}\mathcal{M}(\vec{v})\sum_{0\le \mathbf{l}\le \mathbf{M}} \sigma(\vec{v},\vec{v}^{\mathbf{l}})\varphi(\vec{v}^{\mathbf{l}})\omega^{\mathbf{l}} - \lambda(\vec{v})r(\vec{v})\,,\end{aligned}$$

with the collision frequency

$$\lambda(\vec{v}) = \int_{\mathbb{R}^3} \sigma(\vec{v},\vec{v}')\mathcal{M}(\vec{v}')\mathrm{d}\vec{v}' = \pi^{-3/2}\sum_{0\le \mathbf{l}\le \mathbf{M}} \sigma(\vec{v},\vec{v}^{\mathbf{l}})\omega^{\mathbf{l}}\,.$$

6. Numerical Experiments

In this section, we apply IMUG and IMSG to several transport problems, where the boundary conditions are assumed to be periodic and the cross sections are given as

$$\begin{aligned}&\sigma^{RTA}(\vec{v},\vec{v}') = 1\,,\\ &\sigma^{EPI}(\vec{v},\vec{v}') = \mathcal{M}(\vec{v})\tilde{\delta}(|\vec{v}|^2 - |\vec{v}'|^2 + 1) + \mathcal{M}(\vec{v}')\tilde{\delta}(|\vec{v}|^2 - |\vec{v}'|^2 - 1)\,,\\ &\sigma^{MIX} = \frac{1}{2}(\sigma^{RTA} + \sigma^{EPI})\,,\\ &\sigma^{CON}(\vec{v},\vec{v}') = \mathcal{M}(\vec{v})\tilde{\delta}^*(|\vec{v}|^2 - |\vec{v}'|^2 + 1) + \mathcal{M}(\vec{v}')\tilde{\delta}^*(|\vec{v}|^2 - |\vec{v}'|^2 - 1)\,,\end{aligned}$$

with $\tilde{\delta}(x) = \exp(-|x|^2)$ and $\tilde{\delta}^*(x) = \exp(-|x|)$. Here σ^{RTA} and σ^{EPI} denote the relaxation time approximation and the electron-phonon interactions, respectively [22, 14]. The velocity discretization is done with the moment method introduced in section 5. Since the numerical tests show that the differences between the solutions using larger M and the results using $\mathbf{M} = (16, 16, 16)$ are comparable, hence, we only give the results with $\mathbf{M} = (16, 16, 16)$.

6.1. One Space Dimension. Consider the physical domain $\Omega = [0, 1]$. The norm $\|\cdot\|$ in one space dimension is calculated through

$$\|r\| = \Delta x \sum_{i=0}^{N-1} \sum_{\mathbf{m}}^{\mathbf{M}} |\varphi(x_i, \vec{v}^{\mathbf{m}}, t)| \omega^{\mathbf{m}},$$

where $r = \varphi \mathcal{M} \in \mathcal{H}$ and $\omega^{\mathbf{m}}$ is given by (44).

6.1.1. Accuracy. We verify the accuracy of IMUG and IMSG through Example 1-Example 3, where the reference solutions in Example 2- Example 3 are calculated by the diffusive relaxation schemes [5] being uniformly stable under $\Delta t \sim O(\Delta x^2)$.

Example 1. *Convergence rates of IMUG and IMSG. Consider the constant Knudsen number $\delta(x) = \epsilon$, the cross section σ^{MIX}, and the electric field $E(x) = \cos(2\pi x)$. The non-equilibrium initial conditions are given by*

$$\begin{aligned} r(x, \vec{v}, 0) &= [2 + \cos(2\pi x)](e^{-v_1} + e^{v_1})\mathcal{M}(\vec{v}), \\ j(x, \vec{v}, 0) &= \epsilon^{-1}[2 + \cos(2\pi x)](e^{-v_1} - e^{v_1})\mathcal{M}(\vec{v}). \end{aligned} \tag{45}$$

The relative error $e_{\Delta t}$ at time $T > 0$ is defined by

$$e_{\Delta t}(T) = \max_{T>0} \frac{\|r_{\Delta t}(T) - r_{2\Delta t}(T)\|}{\|r_{2\Delta t}(0)\|}. \tag{46}$$

Here, $r_{\Delta t}$ is obtained with Δx and Δt, while, $r_{2\Delta t}$ is solved with Δx and $2\Delta t$. We present the numerical results in Fig. 1, where $\Delta x = 10^{-3}$ and $\Delta t = \Delta x/2^k$ with $k = 2, 3, 4, 5, 6, 7$. There, we plot $\log_{10} e_{\Delta t}$ at $T = 0.08$ for $\epsilon = 1,\ 10^{-1},\ 10^{-2},\ 2 \times 10^{-3}$, respectively. As a conclusion, both IMUG (which gives Fig. 1(a)) and IMSG (which gives Fig. 1(b)) are first order accurate with respect to Δt.

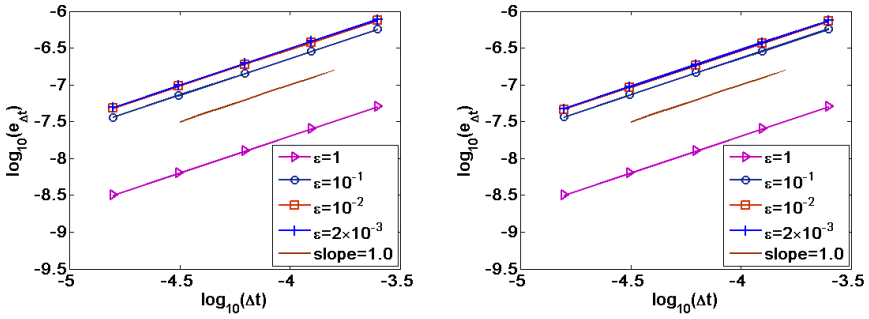

(a) IMUG (b) IMSG

FIGURE 1. Convergence rates of one space dimensional schemes in Example 1. The cross section is σ^{MIX}, the electric field is $E(x) = \cos(2\pi x)$, and the non-equilibrium initial conditions are given by (45). In both Fig. 1(a) and Fig. 1(b), $\log_{10}(e_{\Delta t})$ are plotted at $T = 0.08$ with $\Delta x = 10^{-3}$ and $\Delta t = \Delta x/2^k$, $k = 2, 3, 4, 5, 6, 7$.

Example 2. *Time evolutions of macroscopic observables by IMUG. Consider the varied Knudsen number*

$$\delta(x) = \epsilon_0 e^{-100(x-0.5)^2}, \quad \epsilon_0 = 10^{-1}, \quad 10^{-3}.$$

the cross section $\sigma^{RTA}+\sigma^{EPI}$, *and the electric field* $E(x)=\sin(2\pi x)$. *When* $\epsilon_0=10^{-1}$, *the initial conditions are in the local equilibrium state*

$$r(x,\vec{v},0)=|\cos(2\pi x)|\,,\quad j(x,\vec{v},0)=0\,. \tag{47}$$

When $\epsilon_0=10^{-3}$, *the initial conditions are away from the local equilibrium state*

$$\begin{aligned} r(x,\vec{v},0)&=C_\rho|\cos(2\pi x)|(e^{-v_1}+e^{v_1})\mathcal{M}(\vec{v})\,,\\ j(x,\vec{v},0)&=C_\rho\epsilon^{-1}|\cos(2\pi x)|(e^{-v_1}-e^{v_1})\mathcal{M}(\vec{v})\,, \end{aligned} \tag{48}$$

with

$$C_\rho=\left[\int_{\mathbb{R}^3}(e^{-v_1}+e^{v_1})\mathcal{M}(\vec{v})\mathrm{d}\vec{v}\right]^{-1}.$$

The numerical results are shown in Fig. 2-Fig. 3, where the dash lines denote the initial macroscopic observables generated from (47) *and* (48) *correspondingly. The solid lines are the reference solutions calculated by the diffusive relaxation scheme based on the time-unsplitting technique using* $\Delta x=1/400\,,\Delta t=\Delta x^2/4$. *The approximate solutions "▷", "○", "*" are solved by IMUG using* $\Delta x=1/50\,,\Delta t=\Delta x/10$.

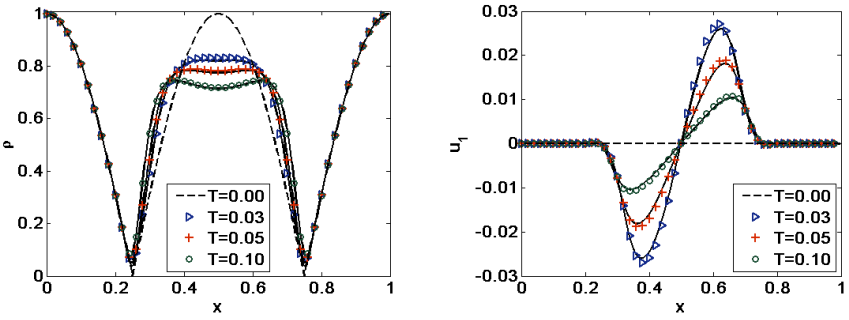

(a) Mass Density (b) Bulk Momentum

FIGURE 2. Time evolutions of ρ and u_1 in Example 2 with the varied Knudsen number $\delta(x)=e^{-100(x-0.5)^2}/10$, the cross section $\sigma^{RTA}+\sigma^{EPI}$, the electric field $E(x)=\sin(2\pi x)$, and the initial conditions (47) in the local equilibrium state. The solid lines are the reference solutions calculated by the diffusive relaxation scheme based on the time-unsplitting technique using $\Delta x=1/400$, $\Delta t=\Delta x^2/4$. The approximate solutions "▷", "○", "*" are solved by IMUG with $\Delta x=1/50\,,\Delta t=\Delta x/10$.

Example 3. *Time evolutions of macroscopic observables by IMSG. Consider* $\delta(x)=\epsilon$ *with* $\epsilon=5\times10^{-1},\,2\times10^{-2}$, *the cross section* $\sigma^{RTA}+\sigma^{CON}$, *the electric field* $E(x)=e^{-50(x-0.5)^2}$, *and the initial data in the local equilibrium state given by*

$$r(x,\vec{v},0)=\mathcal{M}(\vec{v})\,,\quad j(x,\vec{v},0)=0\,. \tag{49}$$

We present the numerical results in Fig. 4, where the dash lines denote the initial macroscopic observables generated by (49). *The solid lines are the reference solutions calculated by the diffusive relaxation scheme based on the time-splitting technique using* $\Delta x=1/400\,,\Delta t=\Delta x^2/4$. *The approximate solutions "▷", "+", "○", "*" are solved by IMSG using* $\Delta x=1/50\,,\Delta t=\Delta x/10$.

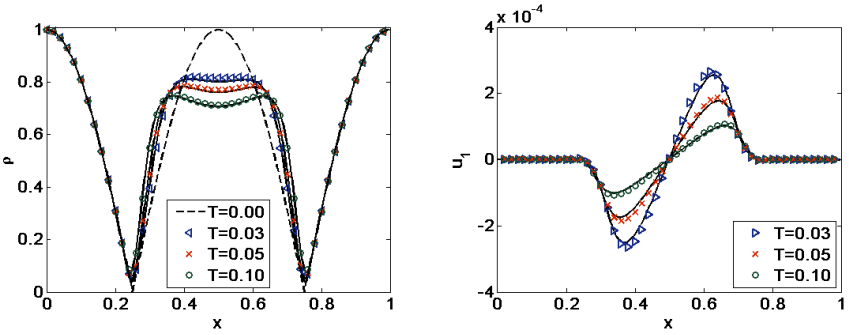

(a) Mass Density (b) Bulk Moentum

FIGURE 3. Time evolutions of ρ and u_1 in Example 2 with the varied Knudsen number $\delta(x) = e^{-100(x-0.5)^2}/1000$, the cross section $\sigma^{RTA} + \sigma^{EPI}$, the electric field $E(x) = \sin(2\pi x)$, and the non-equilibrium initial conditions (48). The solid lines are the reference solutions solved by the diffusive relaxation scheme based on the time-unsplitting technique using $\Delta x = 1/400$, $\Delta t = \Delta x^2/4$. The approximate solutions "$\triangleright$", "$\circ$", "$*$" are solved by IMUG using $\Delta x = 1/50\,, \Delta t = \Delta x/10$.

6.1.2. The AP Property. From right figures in Fig. 2-Fig. 4, both IMUG and IMSU give the bulk momentum u_1 fulfilling $|u_1| \sim O(\epsilon)$, which coincides with the asymptotic analysis in section 2. Next, we verify another two properties, i.e., $r - \rho\mathcal{M} \sim O(\epsilon^2)$ and $\rho - \tilde{\rho} \sim O(\epsilon^2)$, for IMUG and IMSG in the situation of $\delta(\vec{x}) = \epsilon$. The numerical results are shown in Example 4-Example 5.

Example 4. *Given $\delta(x) = \epsilon$ with $\epsilon = 10^{-k}$ and $k = 1\,, 2\,, 3\,, 4\,, 5\,, 6$.*

Case 1 *Consider the cross section σ^{MIX}, the constant electric field $E(x) = 1$, and the initial data in the non-equilibrium state*

$$\begin{aligned} r(x,\vec{v},0) &= e^{-50(x-0.5)^2}(e^{-v_1} + e^{v_1})\,\mathcal{M}(\vec{v})\,, \\ j(x,\vec{v},0) &= \frac{e^{-50(x-0.5)^2}}{\epsilon}(e^{-v_1} - e^{v_1})\mathcal{M}(\vec{v})\,. \end{aligned} \tag{50}$$

Case 2 *Consider the cross section $\sigma^{RTA} + \sigma^{CON}$, the varied electric field $E(x) = \exp[-50(x-0.5)^2]$, and the initial data in the local equilibrium state*

$$r(x,\vec{v},0) = 1.0 + |\sin(2\pi x)|\,, \quad j(x,\vec{v},0) = 0\,. \tag{51}$$

We present the numerical results in Fig. 5- Fig. 6, where $\Delta x = 1/25\,, \Delta t = \Delta x$. In Fig. 5, we consider Case 1 and plot $\log_{10}\|r - \rho\mathcal{M}\|$ at $T = 2.0$. In Fig. 6, we calculate $\log_{10}\|r - \rho\mathcal{M}\|$ at $T = 6.0$ for Case 2. In the two figures, Fig. 5(a) and Fig. 6(a) are calculated by IMUG, while, Fig. 5(b) and Fig. 6(b) are solved by IMSG. As a conclusion, both IMUG and IMSG give the relations $\|r - \rho\mathcal{M}\| \sim O(\epsilon^2)$.

Example 5. *We consider the same conditions as Example 3. We compare the approximate solutions ρ generated by IMUG and IMSG with the reference solution $\tilde{\rho}$ given by the implicit discretization of the drift-diffusion equation* (9)

$$\frac{\tilde{\rho}_i^{n+1} - \tilde{\rho}_i^n}{\Delta t} - \mu\frac{\tilde{\rho}_{i+1}^{n+1} - 2\tilde{\rho}_i^{n+1} + \tilde{\rho}_{i-1}^{n+1}}{\Delta x^2} - \mu\frac{E_{i+1}\tilde{\rho}_{i+1}^{n+1} - E_{i-1}\tilde{\rho}_{i-1}^{n+1}}{\Delta x} = 0\,. \tag{52}$$

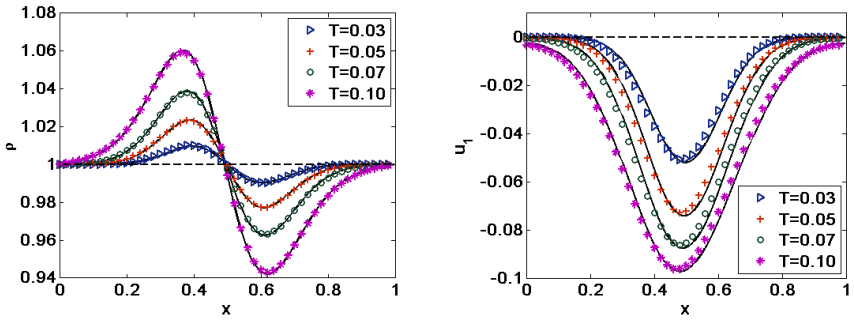

(a) $\epsilon = 5 \times 10^{-1}$

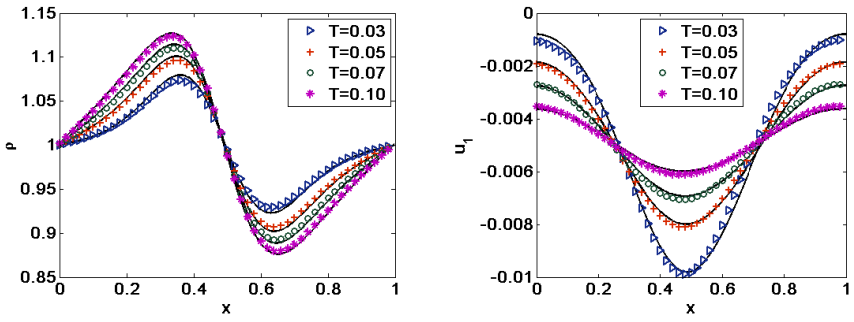

(b) $\epsilon = 2 \times 10^{-2}$

FIGURE 4. Time evolutions of ρ and u_1 in Example 3. The constant Knudsen number $\delta(x) = \epsilon$, the cross section $\sigma^{RTA} + \sigma^{CON}$, the electric field $E(x) = e^{-50(x-0.5)^2}$, and the initial data (49) in the local equilibrium state. The solid lines are solved using the diffusive relaxation scheme based on the time-splitting method with $\Delta x = 1/400$, $\Delta t = \Delta x^2/4$. "▷", "+", "○", "*" are solved using IMSG with $\Delta x = 1/50\,, \Delta t = \Delta x/10$. Left: Mass density. Right: Bulk momentum.

Here, the mobility μ is calculated through

$$\mu = \sum_{0 \le \mathbf{m} \le \mathbf{M}} \frac{(v_1^{m_1})^2 \omega^{\mathbf{m}}}{\lambda(\vec{v}^{\mathbf{m}})}\,, \tag{53}$$

and the initial data

$$\tilde{\rho}_i^0 = \sum_{\mathbf{m}}^{\mathbf{M}} \varphi(x_i, \vec{v}^{\mathbf{m}}, 0)\omega^{\mathbf{m}}\,. \tag{54}$$

The numerical results are shown in Fig. 7, where the solid lines are given by IMUG and the dash lines are solved by IMSG. They describe the time evolutions of $\|\rho - \tilde{\rho}\|_1$ with

$$\|\rho - \tilde{\rho}\|_1 = \Delta x \sum_{i=0}^{N-1} |\rho(x_i, t) - \tilde{\rho}(x_i, t)|\,. \tag{55}$$

In Fig. 7, we solve ρ with $\Delta x = 1/50\,, \Delta t = \Delta x/10$ and $\tilde{\rho}$ with $\Delta x = 1/200\,, \Delta t = \Delta x^2$. According to Fig. 7(a), the drift-diffusion equation can not describe the system

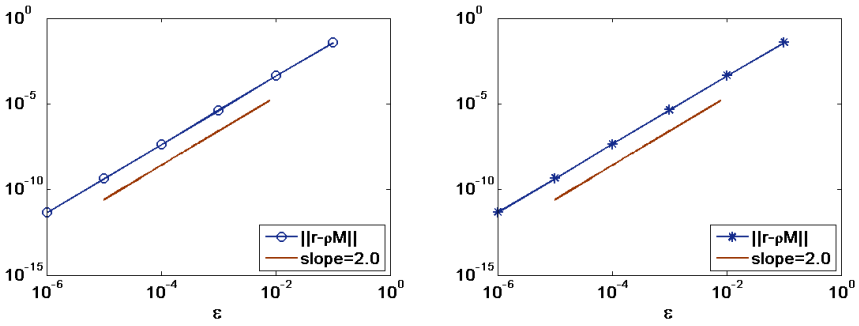

(a) IMUG (b) IMSG

FIGURE 5. AP property of one space dimensional scheme in Example 4. The constant Knudsen number $\delta(x) = \epsilon$, the cross section σ^{MIX}, the electric field $E(x) = 1$, the non-equilibrium initial data (50), and the mesh $\Delta x = 1/25\,, \Delta t = \Delta x$. Both $\log_{10} \|r - \rho\mathcal{M}\|$ in (a) and (b) are obtained at $T = 2.0$.

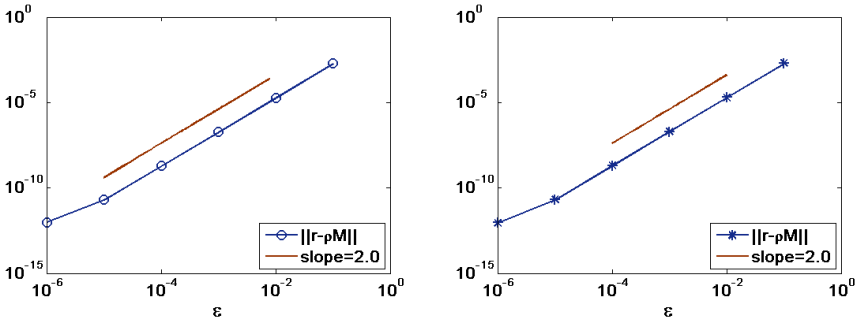

(a) IMUG (b) IMSG

FIGURE 6. AP property of one space dimensional scheme in Example 4 with the constant Knudsen number $\delta(x) = \epsilon$, the cross section $\sigma^{RTA} + \sigma^{CON}$, the electric field $E(x) = \exp[-50(x-0.5)^2]$, the initial data (51) in the local equilibrium state, and the mesh $\Delta x = 1/25\,, \Delta t = \Delta x$. Both $\log_{10} \|r - \rho\mathcal{M}\|$ in (a) and (b) are obtained at $T = 6.0$.

accurately when ϵ is big. While, Fig. 7(b) suggests that both IMUG and IMSG can give the relation $\|\rho - \tilde{\rho}\|_1 \sim O(\epsilon^2)$.

6.1.3. Two Space Dimension. Consider the physical domain $\Omega = [\,0\,,\,1\,]\times[\,0\,,\,1\,]$ and the cross section σ^{MIX} only. We numerically test IMUG in section 4 through Example 6 -Example 8, where $\Delta t \sim O(\Delta x)$. The norm $\|\cdot\|$ in two space dimension is approximated by

$$\|r\| = \Delta x \Delta y \sum_{i=0}^{N-1} \sum_{l=0}^{N-1} \sum_{\mathbf{m}}^{\mathbf{M}} \big|\varphi(x_i, y_l, \vec{v}^{\mathbf{m}}, t)\big| \omega^{\mathbf{m}}\,, \quad \forall r = \varphi\mathcal{M} \in \mathcal{H}\,.$$

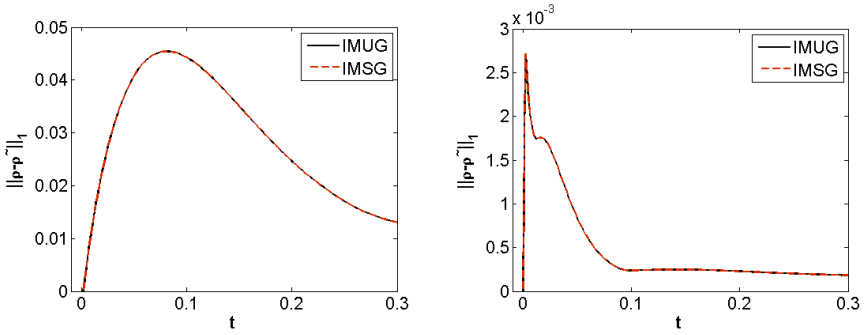

(a) $\epsilon = 5 \times 10^{-1}$ (b) $\epsilon = 2 \times 10^{-2}$

FIGURE 7. Comparisons between the one space dimensional schemes and the drift-diffusion equation in Example 5 with the constant Knudsen number $\delta(x) = \epsilon$, the cross section $\sigma^{RTA} + \sigma^{CON}$, the electric field $E(x) = \exp[-50(x - 0.5)^2]$, and the initial data (49) in the local equilibrium state. ρ is generated by r with $\Delta x = 1/50\,, \Delta t = \Delta x/10$. $\tilde{\rho}$ is obtained from the implicit scheme (52) for the drift-diffusion equation (9) using $\Delta x = 1/200\,, \Delta t = \Delta x^2$.

It can be seen that the numerical results coincide with the diffusion equation, which support the AP property of the scheme.

Example 6. *Consider $\epsilon = 10^{-k}$ with $k = 2, 3, 4, 5, 6$, and the initial conditions in the non-equilibrium state*

$$\begin{aligned} r(x, y, \vec{v}, 0) &= \tilde{C}_\rho \big| \cos(2\pi x) \cos(2\pi y) \big| (e^{-v_1 - v_2} + e^{v_1 + v_2}) \mathcal{M}(\vec{v})\,, \\ j(x, y, \vec{v}, 0) &= \tilde{C}_\rho \epsilon^{-1} \big| \cos(2\pi x) \cos(2\pi y) \big| (e^{-v_1 - v_2} - e^{v_1 + v_2}) \mathcal{M}(\vec{v})\,, \end{aligned} \tag{56}$$

with

$$\tilde{C}_\rho = \left(\int_{\mathbb{R}^3} (e^{-(v_1+v_2)} + e^{v_1+v_2}) \mathcal{M}(\vec{v}) \mathrm{d}\vec{v} \right)^{-1}.$$

We present the numerical results in Fig. 8, where $\log_{10} \|r - \rho\mathcal{M}\|$ are solved at $T = 0.1$ with $\Delta x = 1/50\,, \Delta t = \Delta x/2^k$, $k = 0, 1, 2, 3, 4, 5$. According to Fig. 8(a), there exist a uniform constant $\epsilon_0 > 0$. When $0 < \epsilon \le \epsilon_0$, $\|r - \rho\mathcal{M}\|$ is nearly independent of ϵ. From Fig. 8(b), $\|r - \rho\mathcal{M}\|$ decays with $\epsilon = 10^{-2}$. Both Fig. 8(a) and Fig. 8(b) imply that IMUG is uniformly stable for $\epsilon \le 10^{-2}$ with $\Delta t = \Delta x$.

Example 7. *Consider $\epsilon = 2^k \times 10^{-3}$ with $k = -1, 0, 1, 2, 3$, and the initial conditions around the local equilibrium state*

$$r(x, \vec{v}, 0) = [\,1 + \epsilon \cos(2\pi x) \cos(2\pi y) e^{-(v_1^2 + v_2^2)}\,] \mathcal{M}(\vec{v})\,. \quad j(x, \vec{v}, 0) = 0\,. \tag{57}$$

The numerical results are shown in Fig. 9, where $\Delta x = \Delta y = 1/50$, $\Delta t = \Delta x/8$. The numerical results suggest that IMUG gives the relation $\|r - \rho\mathcal{M}\| \sim O(\epsilon)$.

Example 8. *Consider $\epsilon = 3 \times 10^{-2}, 10^{-3}$, and the initial conditions (57) in the non-equilibrium state. The numerical results are shown in Fig. 10-Fig. 13, where $\Delta x = 1/80\,, \Delta t = \Delta x/10$. In Fig. 10-Fig. 12, we describe the time evolutions of the mass density and the first component of the bulk momentum. Clearly, there establishes $|u_1| \sim O(\epsilon)$. In Fig. 13, we depict the time evolutions of $\|r - \rho\mathcal{M}\|$*

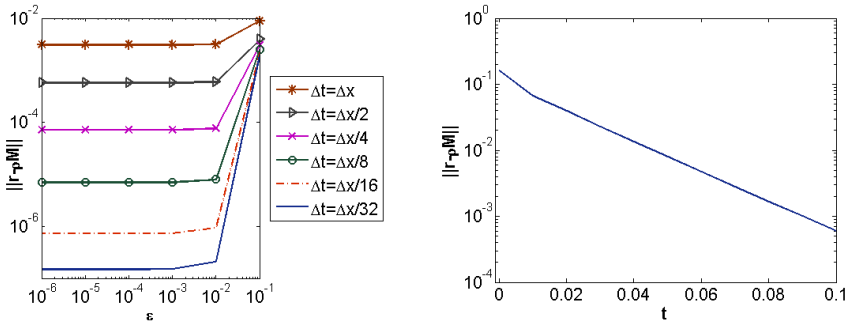

(a) (b)

FIGURE 8. AP property of two space dimensional scheme in Example 6 with constant Knudsen number $\delta(\vec{x}) = \epsilon$, the cross section σ^{MIX}, the electric potential $\Phi(\vec{x}) = 0$, and the non-equilibrium initial data (57). Fig. 8(a) gives $\log_{10} \|r - \rho\mathcal{M}\|$ at $T = 0.1$ with $\epsilon \leq 1e-2$ and $\Delta x = 1/50$. Fig. 8(b) describes the time evolutions of $\log_{10} \|r - \rho\mathcal{M}\|$ with $\epsilon = 1e-2$ and $\Delta x = 1/50\,, \Delta t = \Delta x$.

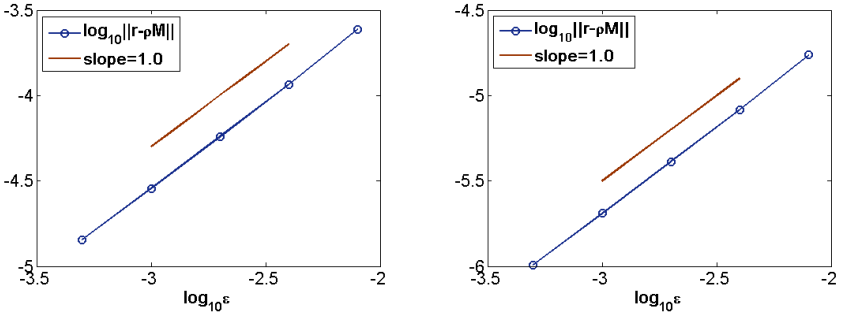

(a) $\log_{10} \|r - \rho\mathcal{M}\|$ at $T = 0.025$ (b) $\log_{10} \|r - \rho\mathcal{M}\|$ at $T = 0.1$

FIGURE 9. AP property of two space dimensional scheme in Example 7 with constant Knudsen number $\delta(\vec{x}) = \epsilon$, the cross section σ^{MIX}, the electric potential $\Phi(\vec{x}) = 0$, the initial conditions (57) around the local equilibrium state, and the mesh $\Delta x = 1/50\,, \Delta t = \Delta x/8$.

(which is denoted by the solid lines) and $\|\rho - \tilde{\rho}\|_1$ *(which is denoted by the dash lines), where* $\tilde{\rho}$ *is solved by*

$$\frac{\tilde{\rho}_{i,l}^{n+1} - \tilde{\rho}_{i,l}^{n}}{\Delta t} - \mu \frac{\tilde{\rho}_{i+2,l}^{n+1} - 2\tilde{\rho}_{i,l}^{n+1} + \tilde{\rho}_{i-2,l}^{n+1}}{4\Delta x^2} - \mu \frac{\tilde{\rho}_{i,l+2}^{n+1} - 2\tilde{\rho}_{i,l}^{n+1} + \tilde{\rho}_{i,l-2}^{n+1}}{4\Delta y^2} = 0\,. \tag{58}$$

Here μ *and* $\tilde{\rho}^0$ *are calculated in the same manner as* (53) *and* (54)*, respectively. The discrete norm* $\|\cdot\|_1$ *in the two space dimension is approximated by*

$$\|\rho - \tilde{\rho}\|_1 = \Delta x \Delta y \sum_{i=0}^{N-1} \sum_{l=0}^{N-1} |\rho(x_i, y_l, t) - \tilde{\rho}(x_i y_l, , t)|\,.$$

The dash lines in Fig. 13 represent $\log_{10}\|\rho-\tilde{\rho}\|_1$*, where* $\log_{10}\|\rho-\tilde{\rho}\|_1$ *at T=0 is numerically set as* $\log_{10}\|\rho-\tilde{\rho}\|_1 = 10^{-14}$*. As a conclusion, the system tends to the global equilibrium state and the mass density* ρ *evolves towards* $\tilde{\rho}$*.*

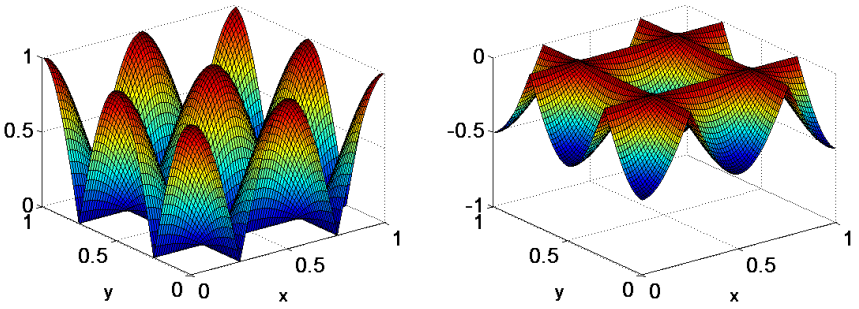

(a) Mass density ρ

(b) The first component u_1 of bulk momentum

FIGURE 10. Initial conditions generated by (56) of two space dimensional system in Example 8.

7. Conclusion

This paper designs the asymptotic-preserving schemes leading to the implicit discretizations of the drift-diffusion equation. The constructions are based on the BGK-penalty method and a suitable implicit approximation to the convection terms, which are decoupled with the correlations among the velocity variables through splitting the system into a stiff relaxation step and a stiff convection step. The BGK-penalty method has the effect of implementing the complicated nonlocal anisotropic collision operator explicitly and meanwhile ensuring the uniform stability of the scheme. The implicit scheme to the convection step gives the banded matrix easy to invert and meanwhile allows $\Delta t = O(\Delta x)$. Through the von-Neumman analysis for the Goldstein-Taylor model, the one space dimensional schemes are unconditionally stable. According to the heuristic discussions, all the proposed schemes are consistent with the implicit discretization of the drift-diffusion equation. Finally, the numerical results support the AP property of the schemes in this paper.

Acknowledgments

The author is grateful to Professor S. Jin for helpful discussions and suggestions. This work is partially supported by the National Natural Science Foundation grant No. 11971115.

References

[1] N. B. Abdallah and P. Degond. On a hierarchy of macroscopic models for semiconductors. *J. Math. Phys.,* 37(7):3306–3333, 1996.

[2] N. B. Abdallah, P. Degond and S. Genieys. An energy-transport model for semiconductors derived from the Boltzmann equation. *J. Static. Phys.,* 84(1-2):205–231, 1996.

[3] G. Bal and Y. Maday. Coupling of transport and diffusion models in linear transport theory. *Math. Model. Numer. Anal.,* 36(1):69–86, 2002.

[4] P. Degond and S. Jin. A smooth transition model between kinetic and diffusion equations. *SIAM J. Numer. Anal.,* 42(6):2671–2687, 2005.

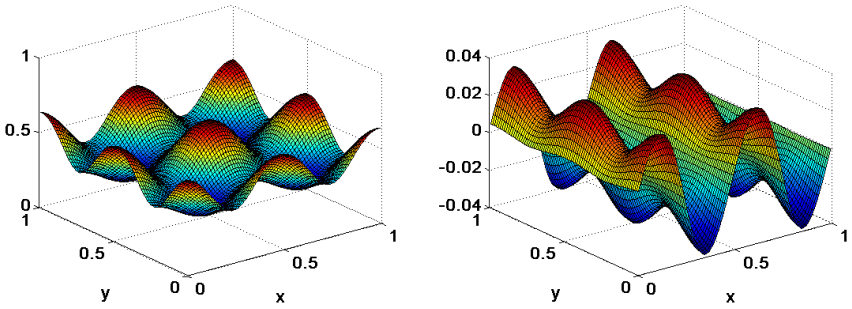

(a) $T = 0.01$

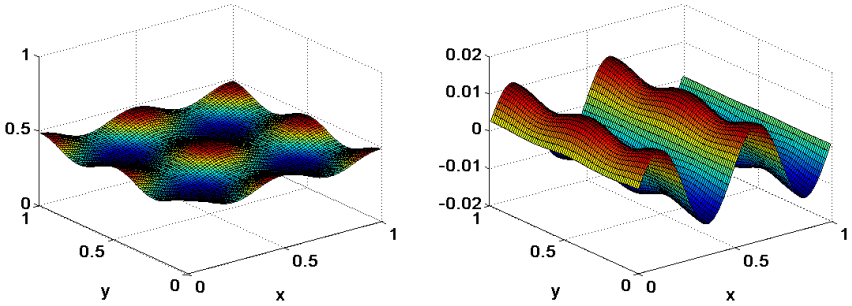

(b) $T = 0.02$

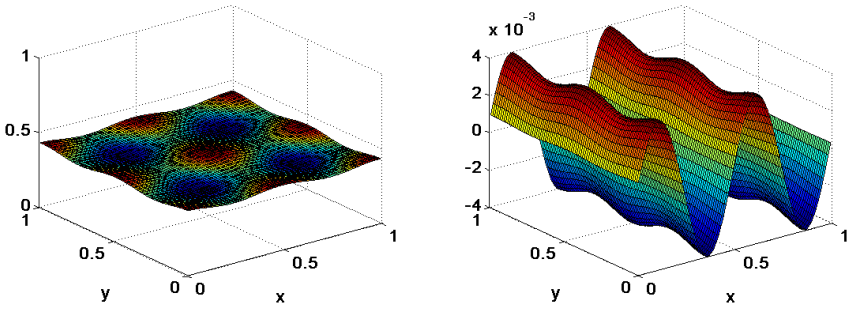

(c) $T = 0.03$

FIGURE 11. Time evolutions of ρ and u_1 by two space dimensional schemes in Example 8. Here, the constant Knudsen number is $\epsilon = 3 \times 10^{-2}$, the cross section is given as σ^{MIX}, the electric field is zero due to $\Phi(x) = 0$, and the initial conditions (57) are in the non-equilibrium state. The space and time steps are set as $\Delta x = 1/80$, $\Delta t = \Delta x/10$. Left: Mass Density ρ. Right: The first component u_1 of the bulk momentum.

[5] J. Deng. Asymptotic preserving schemes for semiconductor Boltzmann equation in the diffusive regime. *Numer. Math. Theor. Meth. Appl.,* preprint.
[6] F. Filbet, J. W. Hu and S. Jin. A numerical scheme for the quantum Boltzmann equation with stiff collision terms. *Math. Model Num. Anal.,* 46, 443–463, 2012.
[7] F. Filbet and S. Jin. A class of asymptotic preserving schemes for kinetic equations and related problems with stiff sources. *J. Comput. Phys.,* 229(20):7625–7648, 2010.

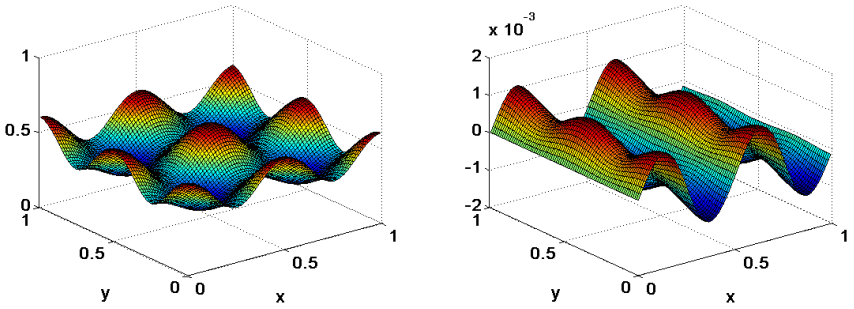

(a) $T = 0.01$

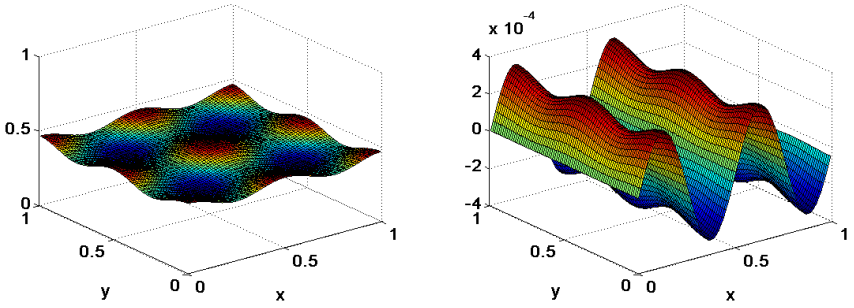

(b) $T = 0.02$

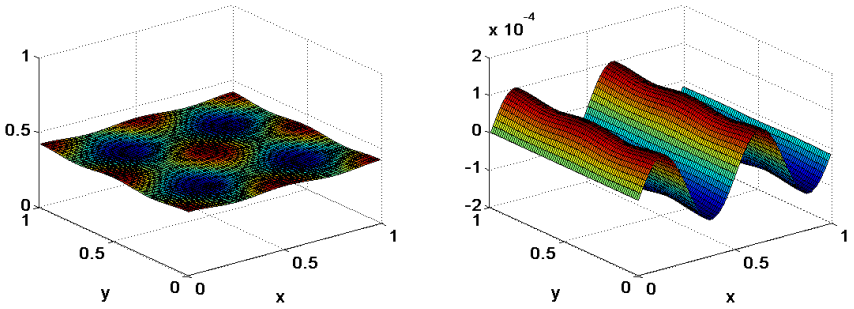

(c) $T = 0.03$

FIGURE 12. Time evolutions of ρ and u_1 by two space dimensional schemes in Example 8. Here, the constant Knudsen number is $\epsilon = 10^{-3}$, the cross section is given as σ^{MIX}, the electric field is zero due to $\Phi(x) = 0$, and the initial conditions (57) are in the non-equilibrium state. The space and time steps are set as $\Delta x = 1/80$, $\Delta t = \Delta x/10$. Left: Mass Density ρ. Right: The first component u_1 of the bulk momentum.

[8] S. Goldstein. On diffusion by discontinuous movements, and on the telegraph equation. *Quart. J. Mech. Appl. Math.,* 4, 129–156, 1951.

[9] F. Golse, S. Jin and C. D. Levermore. A domain decomposition analysis for a two-scale linear transport problem. *M2AN Math. Model. Numer. Anal.,* 37(6):869–892, 2003.

[10] J. W. Hu, S. Jin and B. K. Yan. A numerical scheme for the quantum Fokker-Planck-Landau equation efficient in the fluid regime. *Math. Model Num. Anal.,* 46, 443–463, 2012.

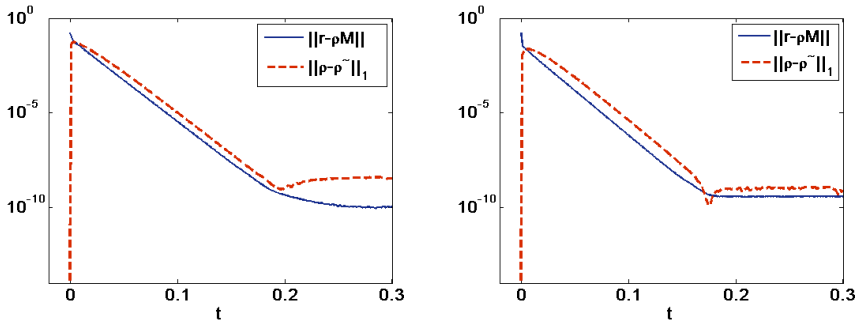

(a) $\epsilon = 3 \times 10^{-2}$ (b) $\epsilon = 10^{-3}$

FIGURE 13. Time evolutions of $\log_{10} \|r - \rho\mathcal{M}\|$ and $\log_{10} \|\rho - \tilde{\rho}\|_1$ bu two space dimensional scheme in Example 8. ρ is generated by r, while, $\tilde{\rho}$ is calculated from the implicit discretization (58) of the diffusion equation. The Knudsen number is constant, the cross section is given as σ^{MIX}, the electric field is zero due to $\Phi(x) = 0$, and the initial conditions (57) are in the non-equilibrium state. The space and time steps are set as $\Delta x = 1/80$, $\Delta t = \Delta x/10$.

[11] S. Jin. Effiient asymptotic preserving (ap) schemes for some multiscale kinetic equations. *SIAM J. Sci. Comput.,* 21(2):441–454 (electronic), 1999.
[12] S. Jin and C. D. Levermore. The discrete-ordinate method in diffusive regimes. *Transport Theory Statist. Phys.,* 20(5-6):413–439, 1991.
[13] S. Jin and C. D. Levermore. Fully discrete numerical transfer in diffusive regimes. *Transport Theory Statist. Phys.,* 22(6):739–791, 1993.
[14] S. Jin and L. Pareschi. Discretization of the multiscale semiconductor Boltzmann equation by diffusive relaxation schemes. *J. Comput. Phys.,* 161(1):312–330, 2000.
[15] S. Jin, L. Pareschi and G. Toscani. Dissusive relaxation schemes for multiscale discrete velocity kinetic equations. *SIAM J. Numer. Anal.,* 35(6):2405–2439, 1998.
[16] S. Jin, L. Pareschi and G. Toscani. Uniformly accurate diffusive relaxation schemes for multiscale transport equations. *SIAM J. Numer. Anal.,* 38(3):913–936(electronic), 2000.
[17] S. Jin and B. K. Yan. A class of asymptotic-preserving schemes for the Fokker-Planck-Landau equation. *J. Comp. Phys.,* 230:6420–6437, 2011.
[18] A. Klar. Asymptotic-induced domain decomposition methods for kinetic and drift diffusion semiconductor equations. *SIAM J. Sci. Comput.,* 19(6):2032–2050(electronic), 1998.
[19] A. Klar. A numerical method for kinetic semiconductor equations in the drift-diffusion limit. *SIAM J. Sci. Comput.,* 20(5):1696–1712(electronic), 1999.
[20] M. Lemou and L. Mieussens. A new asymptotic preserving scheme based on micro-macro formulation for linear kinetic equations in the diffusion limit. *SIAM J. Sci. Comput.,* 31(1):334–368, 2008.
[21] J. G. Liu and L. Mieussens. Analysis of an asymptotic preserving scheme for linear kinetic equations in the diffusion limit. *SIAM J. Numer. Anal.,* 48(4):1474–1491, 2010.
[22] P. A. Markowich, C. A. Ringhofer and C. Schmeiser. Semiconductor Equations. *Springer-Verlag, Vienna.,* 1990.
[23] F. Poupaud and J. Soler. Papabolic limit and stability of the vlasov-fokker-plank system. *Math. Models Methods Appl. Sci.,* 10(7):1027–1045, 2000.
[24] C. Ringhofer, C. Schmeiser and A. Zwrichmayr. Moment methods for the semiconductor Boltzmann equation on bounded position domains. *SIAM J. Numer. Anal.,* 39(3):1078–1095 (electronic), 2001.
[25] C. Schmeiser and A. Zwrichmayr. Convergence of moment methods for linear kinetic equations. *SIAM J. Numer. Anal.,* 36(1):74–88(electronic), 1999.
[26] G. I. Taylor. Diffusion by continuous movements. *J. Math. and Phys.,* 38:36–41, 1959/1960.

[27] M. Tidriri. New models for the solution of intermediate regimes in transport theory and radiative transfer: existence theory, positivity, asymptotic analysis, and approximations. *J. Statist. Phys.,* 104(1-2):291–325, 2001.

[28] X. Yang, F. Golse, Z. Huang and S. Jin. Numerical study of a domain decomposition method for a two-scale linear transport equation. *Netw. Heterog. Media.,* 1(1), 143–166, 2006.

First Institute of Oceanography, State Oceanic Administration, Qingdao, Shandong 266061, China

E-mail: dengj@fio.org.cn